Evanescent-Mode Filters with Arbitrarily Positioned Ridges in Circular Waveguide

Seng Yong Yu and Jens Bornemann
Department of Electrical and Computer Engineering, University of Victoria, BC, Canada
syyu@ece.uvic.ca

Abstract

The design of new circular waveguide evanescent-mode filters is facilitated by an eigenvalue approach which allows an arbitrary number of ridges to be placed at arbitrary locations within a circular waveguide cross sections. Several four-pole filter examples with passbands in the 7 GHz to 10 GHz range include double ridges, T-septa and key-shaped inserts. Although higher-order-mode excitation is observed in the larger input and output guides, their levels are low enough to refrain from influencing the operation of the filters. The performance is validated by comparison with measurements and the commercial full-wave field solver CST Microwave Studio

1. Introduction

The evanescent-mode filter is a well known approach in rectangular waveguide technology, e.g. [1]–[3], for the miniaturization and stopband enhancement of waveguide filters. They require a transition from larger input/output guides to a smaller waveguide which is operated below cutoff. Ridges are implemented at certain locations within the smaller waveguide. They act as resonators by lowering the cutoff frequency of the smaller waveguide to approximately that of the larger connected waveguides. Whereas the evanescent-mode filter concept has found several applications within rectangular waveguides, its counterpart in the circular waveguide housing has so far been employed only sparsely, e.g. [4].

Therefore, this paper proposes new circular waveguide evanescent-mode filter designs with different cross sections whose reliable mode-sequence calculations become possible by a recently developed eigenvalue mode-spectrum analysis [5]. This technique allows the placement of arbitrary numbers of ridges at arbitrary locations within a circular waveguide cross section and thus opens new possibilities for circular waveguide component design. Due to the reduction in cutoff frequency, the ridged cross sections are foremost employable in evanescent-mode-filters and offer a considerable extension of the upper stopband compared to, e.g., circular waveguide iris filters in [6].

In combination with the standard mode-matching technique (MMT), the eigenvalue mode-spectrum analysis becomes a fast and reliable tool for circular waveguide evanescent-mode filter design. After briefly describing the theory and verifying the underlying software code in Section 2, Section 3 presents designs of four different filter configurations.

2. Theory

Fig. 1 shows the cross section of a circular waveguide with three arbitrarily positioned ridges whose locations and sizes are characterized by coordinates (ρ_i, ϕ_i) and cross-section dimensions ($\Delta\rho_i$, $\Delta\phi_i$), respectively. Note that the ridges are of a shape that they are defined in the circular coordinate system. This is a common approach in circular waveguide technology, e.g. [4], [7] – [11]. In order to avoid the TEM mode, restrictions are placed such that individual ridges must be connected to the circular housing or to each other with at least one of them connected to the housing.

The basic eigenvalue approach presented in [12], [13] is translated to the circular-cylindrical coordinate system. Then the mode spectrum of a circular waveguide with N conical ridges (Fig. 1) is obtained by expanding the longitudinal field components of TE and TM modes as

$$H_z = \sum_{q=1}^{Q} c_q h_{zq} \ , \ E_z = \sum_{p=1}^{P} c_p e_{zp} \qquad (1)$$

Instead of using polynomial approximation and super-quadratic functions [13], we select the modes of the circular housing, or modifications thereof, as basis functions. Those of the TE modes

978-1-4577-0253-2/11/$26.00 ©2011 IEEE

$$h_{zq(m,n)} = J_m\left(k_{chmn}\rho\right)\begin{Bmatrix} cos(m\phi)/\sqrt{1+\delta_{0m}} \\ sin(m\phi) \end{Bmatrix} \quad (2)$$

satisfy the bounday conditions for the TE modes in the ridged circular waveguide.

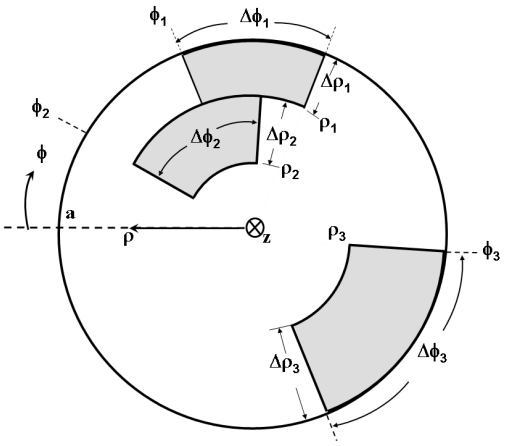

Figure 1. Cross section of a circular waveguide with three arbitrarily positioned ridges.

For TM modes, however, the longitudinal electric field must be forced to vanish over the cross sections of the ridges. This is achieved by a two-dimensional constraint function U which sets e_{zp} in (3) to zero over the cross sections of all N ridges.

$$e_{zp(m,n)} = J_m\left(k_{cemn}\rho\right)\begin{Bmatrix} sin(m\phi) \\ cos(m\phi)/\sqrt{1+\delta_{0m}} \end{Bmatrix} \times\prod_{i=1}^{N} U\left(\frac{\rho-\rho_i}{\Delta\rho_i},\frac{\phi-\phi_i}{\Delta\phi_i}\right) \quad (3)$$

$$U\left(\frac{\rho-\rho_i}{\Delta\rho_i},\frac{\phi-\phi_i}{\Delta\phi_i}\right) = \begin{cases} 0 & \begin{cases} \text{if} & \rho_i \le \rho \le \rho_i+\Delta\rho_i \\ \text{and} & \phi_i \le \phi \le \phi_i+\Delta\phi_i \end{cases} \\ 1 & \text{otherwise} \end{cases} \quad (4)$$

In (2), and (3), J_m are the Bessel functions of first kind and order m; k_{ch} and k_{ce} are the cutoff wave numbers of TE and TM modes, respectively, in the circular waveguide housing; and δ_{0m} is the Kronecker delta. Note that the derivatives of (3) contain delta functions which are considered using the sifting theorem. For details, the reader is referred to [5].

The eigenvalue matrices $\underline{k_c}$ of the TE and TM modes of the ridged circular waveguide, and their respective eigenvector matrices $\underline{c}$, are obtained from a classical eigenvalue equation

$$K\underline{c} = \underline{k_c}^2 M\underline{c} \quad (5)$$

where matrices K and M are given in [5]. Since the coupling matrices from the circular housing to the circular ridged waveguide as well as power normalizations follow straightforwardly, this approach lends itself to be immediately incorporated in an MMT code. The interested reader will find in [5] the complete set of equations, including the combination of the eigenvalue mode-spectrum analysis with MMT and related coupling integrals. We refrain from reproducing this work.

In order to verify the underlying code in a filter arrangement, Fig. 2 shows a comparison of this method with measurements presented in [14]. Considering the facts that the measurements include rectangular to circular waveguide tapers at both ports and that the theoretically assumed conical septum shape was actually fabricated by etching a thin sheet of metal, the agreement is excellent and validates the analysis concept presented in this section.

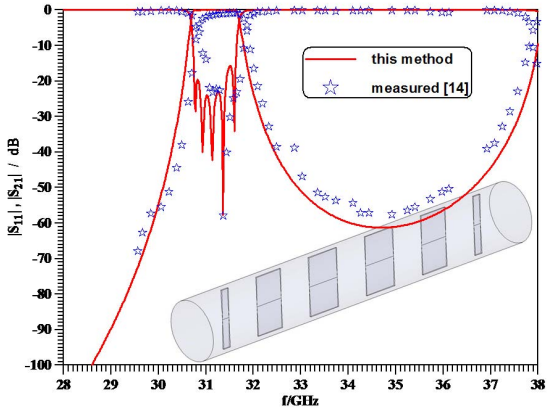

Figure 2. Performance of a five-resonator metal-insert filter in circular waveguide technology. Comparison of results obtained with this method and measurements [14].

The design of circular waveguide evanescent-mode filters proceeds as follows. Based on the midband frequency of the filter and the respective radius of the input/output guides, the small waveguide radius (c.f. inset of Fig. 3) is selected such that its cutoff frequency is sufficiently above the midband frequency of the filter. The ridges are designed to reduce the fundamental-mode cutoff frequency of the small waveguide to approximate that of the larger input/output waveguides. We then compute the scattering matrix of the discontinuity between the circular waveguide filled with ridges and the empty small waveguide which is operated below cutoff. This information is used with [15] to calculate the resonant lengths of the ridged waveguide resonators including the adjacent evanescent-mode sections. Only the input

and output discontinuities cannot be covered through the procedure in [15]. Therefore, the length between this discontinuity and the first ridged resonator is varied first in a one-dimensional optimization. A fine optimization of all filter section lengths completes the design.

3. Results

Several four-pole circular waveguide evanescent-mode filters have been designed using this method. In all examples, the below-cutoff waveguide has a diameter of 13.0 mm so that its cutoff frequency is 13.5 GHz. As input/output guides, standard circular waveguides WC94, WC109 or WC128 with cutoff frequencies of 7.4 GHz, 6.3 GHz and 5.4 GHz, respectively, are selected.

Fig. 3 shows the performance of a double-ridged waveguide filter centered at 9.5 GHz. Note that the cross section is two-plane symmetric and, therefore, higher-order modes in the WC109 input/output guides appear at 13.16 GHz and 14.43 GHz due to that symmetry. However, the conversion to these two modes is below -60 dB up to 16 GHz and thus is sufficient in many practical applications. A comparison with the commercial software package CST Microwave Studio shows excellent agreement up to 12 GHz. Some discrepancy is observed for the region in which higher-order modes occur. Here CST appears to sum up the power carried by individual modes whereas MMT distinguishes between them. As for a CPU-time comparison, the

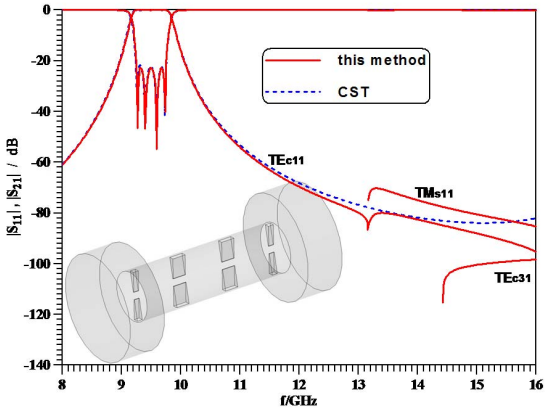

Figure 3. Performance of a four-pole evanescent-mode filter in double-ridged circular waveguide technology and comparison with results obtained from CST Microwave Studio.

eigenvalue method combined with an MMT code outperforms CST depending on the number of frequency samples required. For 250, 500 and 1000 frequency points, the eigenvalue method is faster than CST by a factor of more than 3, 6 and 10, respectively.

The performance of a filter in circular T-septum waveguide technology centered at 9.0 GHz is shown in Fig. 4. Although the input/output guides (WC94) are smaller compared to those of the filter in Fig. 3, the single-plane symmetry of the cross section produces a different set of higher-order modes. However, their excitation is below -60 dB up to almost 15 GHz.

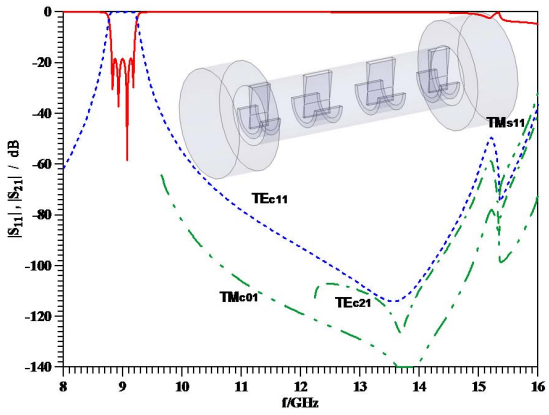

Figure 4. Performance of a four-pole evanescent-mode filter in circular T-septum waveguide technology.

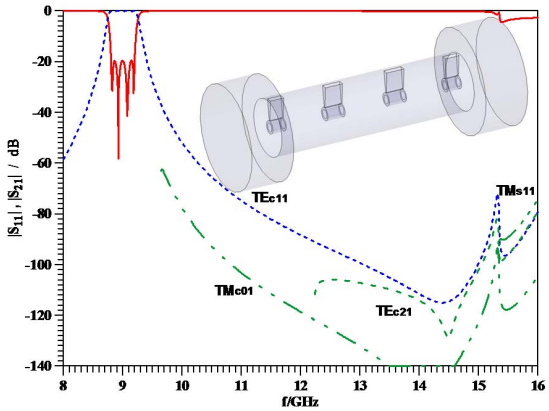

Figure 5. Performance of a four-pole evanescent-mode filter in circular key-shaped ridged waveguide technology.

A comparable filter in circular key-shaped ridged waveguide technology is depicted in the inset of Fig. 5. This cross section emerged from a single circular T-septum configuration, in which the two arms of the T-bar have been extended to reduce the cross section's cutoff frequency, until the ring was completed. It is interesting to note that the mode

spectrum of the key-shaped cross section contains as a subset that of the small center circular waveguide. The performance of this filter (Fig. 5) is similar to that of Fig. 4 but the excitation of higher-order mode magnitudes is reduced, thus providing a better stopband behavior towards higher frequencies.

The final example is an evanescent-mode filter in circular double-T-septum waveguide technology as shown in Fig. 6. The WC128 input/output guides are larger than in the previous examples because they need to facilitate proper propagation around the filter's midband frequency of 7.2 GHz. Due to the double-plane cross-section symmetry, a higher-order mode set similar of that in Fig. 3 is excited, but individual contributions are at levels at or below -90 dB up to 16 GHz. This is certainly the best filter performance of the examples shown here.

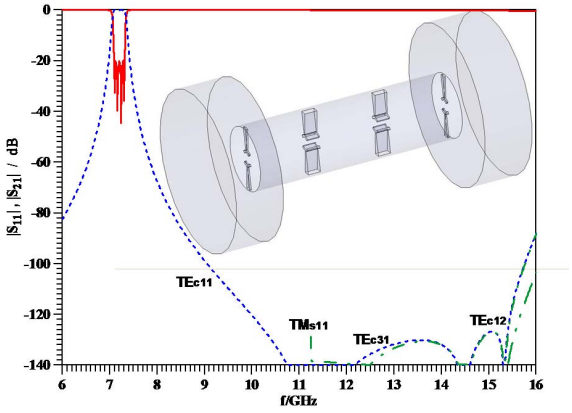

Figure 6. Performance of a four-pole evanescent-mode filter in circular double-T-septum waveguide technology.

It is noted that a configuration similar to that of Fig. 6 was built and measured in rectangular double-T-septum waveguide technology. The results and a direct comparison with this technique are reported in [16] and thus not repeated here. A direct comparison with a measured circular evanescent-mode filter similar to that of Fig. 3 is also shown in [16]. These filters exhibit measured in-band insertion losses of about 2 -3 dB which is what we would expect for the filter in Fig. 6 as well.

4. Conclusions

The new circular waveguide evanescent-mode filters with arbitrarily positioned ridges present a viable option for stand-alone circular waveguide bandpass filters. Compared to circular waveguide iris filters, they achieve component miniaturization and an extended stopband towards higher frequencies. The utilization of the new cross sections is facilitated by employing a classical eigenvalue mode-spectrum analysis which allows varying numbers of metallic inserts in the circular waveguide's cross section to be considered at arbitrary locations. This provides an opportunity for new circular waveguide component designs. The double-T-septum filter with the best performance is expected to produce insertion losses of about 2.0-2.5 dB due to its miniaturization compared to ordinary circular waveguide bandpass filters.

5. References

[1] G. Craven and C.K. Mok, "The design of evanescent mode waveguide band-pass filters for a prescribed insertion loss characteristic," *IEEE Trans. Microwave Theory Tech.*, vol. 19, no. 3, Mar. 1971, pp. 295-308.

[2] H.F. Chappell, "Waveguide low pass filter using evanescent mode inductors," *Microwave J.*, vol. 21, no. 12, Dec. 1978, pp. 71–72.

[3] V.A. Labay and J. Bornemann, "CAD of T-septum waveguide evanescent-mode filters," *IEEE Trans. Microwave Theory Tech.*, vol. 41, no. 4, Apr. 1993, pp. 731-733.

[4] J. Huang, R. Vahldieck, and H. Jin, "Computer-aided design of circular ridged waveguide evanescent-mode bandpass filters using the FDTLM method," *IEEE MTT-S Int. Microwave Symp. Dig.*, June 1993, pp. 459-462.

[5] S.Y. Yu and J. Bornemann, "Classical eigenvalue mode-spectrum analysis of multiple ridged rectangular and circular waveguides for the design of narrowband waveguide components," *Int. J. Numer. Model.*, Vol. 22, pp. 395-410, Nov./Dec. 2009.

[6] J. Bornemann and S. Amari, "Improved waveguide filters for applications involving circular polarization," *IEEE AP-S Int. Symp. Dig.*, July 2001, pp. 278-281.

[7] J. Bornemann, S. Amari, J. Uher, and R. Vahldieck, "Analysis and design of circular ridged waveguide components," *IEEE Trans. Microwave Theory Tech.*, vol. 47, no. 3, Mar. 1999, pp. 330-335.

[8] H.Z. Zhang and G.L. James, "Characteristics of quad-ridged coaxial waveguides for dual-band horn applications," *IEE Proc.-Microw. Antennas Propag.*, vol. 145, no. 3, June 1998, pp. 225-228.

[9] H.Z. Zhang, "A wideband orthogonal-mode junction using a junction of a quad-ridged coaxial waveguide and four sectoral waveguides," *IEEE Microwave Wireless Comp. Lett.*, vol. 12, no. 5, May 2002, pp. 172-174.

[10] A.E. Serebryannikov, O.E. Vasylchenko, and K. Schünemann, "Fast coupled-integral-equations-based analysis of azimuthally corrugated cavities," *IEEE Microwave Wireless Comp. Lett.*, vol. 14, no. 5, May 2004, pp. 240-242.

[11] A. Morini, T. Rozzi, and A. Angeloni, "Accurate calculation of the modes of the circular multiridge waveguide," *IEEE MTT-S Int. Microwave Symp. Dig.*, June 1997, pp. 199-202.

[12] S.-L. Lin, L.-W. Li, T.-S. Yeo, and M.-S. Leong, "Cutoff wavenumbers in truncated waveguides," *IEEE Microwave Wireless Comp. Lett.*, vol. 11, no. 5, May 2001, pp. 214-216.

[13] S.-L. Lin, L.-W. Li, T.-S. Yeo, and M.-S. Leong, "Analysis of metallic waveguides of a large class of cross sections using polynomial approximation and superquadratic functions," *IEEE Trans. Microwave Theory Tech.*, vol. 49, no. 6, June 2001, pp. 1136-1139.

[14] B. V. de la Filolie, *Field theory analysis of rectangular and circular waveguide discontinuities for filters, multiplexers and matching networks*, PhD Dissertation, University of Victoria, 1992.

[15] S. Amari, J. Bornemann and R. Vahldieck, "A technique for designing ring and rod dielectric resonators in cutoff waveguides," *Microwave Opt. Technol. Lett.*, vol. 23, no. 4, Nov. 1999, pp. 203-205.

[16] S.Y. Yu and J. Bornemann, "Polarization-preserving evanescent-mode filters", *Microwave Opt. Technol. Lett.*, vol. 53, pp. 1435-1439, June 2011.